

# Evidence for external forcing on 20th-century climate from combined ocean-atmosphere warming patterns

Jan Sedláček<sup>1</sup> and Reto Knutti<sup>1</sup>

Received 24 July 2012; revised 18 September 2012; accepted 19 September 2012; published 23 October 2012.

[1] Of the additional energy absorbed by the Earth over the past decades, by far the largest fraction is taken up by the oceans. Yet most attribution studies focus on the surface warming, and only few have used patterns of ocean warming to attribute changes to external forcing or internal variability. Here we use the combined observed evidence from warming of the atmosphere and ocean with the latest climate model simulations to demonstrate that both the depth profiles and spatial warming patterns near the surface are very heterogeneous when resulting from internal unforced variability. In the 20th-century simulations on the other hand, the observed spatial pattern is smooth, and the warming decreases almost gradually with depth in the ocean, consistent with observations and a penetration of the surface warming to intermediate depth by diffusion and advection. We argue that such physically motivated arguments combining different lines of evidence and types of observations offer insight that is complementary to optimal fingerprint attribution methods. We conclude that the simultaneous global warming of the atmosphere and mixed layer alone is uninformative for attribution, but the magnitude of ocean heat uptake, the homogeneity of the spatial pattern as well as the distribution of warming below the mixed layer strongly argue for the 20th-century warming being largely externally forced. **Citation:** Sedláček, J., and R. Knutti (2012), Evidence for external forcing on 20th-century climate from combined ocean-atmosphere warming patterns, *Geophys. Res. Lett.*, 39, L20708, doi:10.1029/2012GL053262.

## 1. Introduction

[2] Attribution of observed trends to causes is a cornerstone in a chain of arguments for human-induced climate change. Traditionally, detection and attribution of the observed 20th-century warming to anthropogenic or natural forcing, or internal unforced variability is done by optimal fingerprinting, a statistical regression method which essentially projects observations onto simulated patterns from single forcing model simulations [Hasselmann, 1979]. These methods demonstrate with very high confidence that most of the observed surface warming since 1950 is of anthropogenic origin [Hegerl *et al.*, 2007], largely based on the argument that the patterns resulting from different forcings are distinct.

While powerful and statistically rigorous, these attribution methods are not intuitive for non-experts. Usually the surface patterns in the atmosphere, or the vertical structure, or the ocean are considered in isolation. Optimal fingerprinting also requires assumptions about linearity when scaling patterns of change, and about the magnitude of internal variability, which typically is derived from model simulations. Whether climate models capture all aspects of multi-decadal internal unforced variability is still debated [Swanson *et al.*, 2009]. The Atlantic Multi-decadal Oscillation (AMO) for example has recently been invoked in various publications as an explanation for parts of the observed changes [DelSole *et al.*, 2011; Huss *et al.*, 2009] but its effect in models is small. Separating internal from forced variability is difficult, however, and part of the discrepancy between models and observations may be due to incomplete forcings in models [Booth *et al.*, 2012].

[3] Another argument for a strong anthropogenic influence on climate, independent of patterns, comes from understanding the basic physical principles of the greenhouse effect, from estimates of the response of temperature to greenhouse gases based on various lines of evidence [Knutti and Hegerl, 2008], and knowledge about changes in radiative forcing and the global energy balance over the instrumental period [Huber and Knutti, 2011]. Here we argue that these arguments can be complemented by looking model simulated patterns of change without necessarily invoking a complex fingerprint method. In particular, we argue that the combined evidence of warming in the atmosphere and ocean, and the horizontal and vertical structure of the ocean warming is consistent with a dominant external and rather smoothly increasing forcing, and inconsistent with internal variability alone. Simple physical arguments can explain the differences between unforced and forced variability. Because the arguments can be made based on normalized patterns rather than magnitudes of change, a potential underestimation of multi-decadal variability in climate models [Gleckler *et al.*, 2012] is unlikely to question the results presented here. The magnitude of change further increases the confidence for dominant external cause.

[4] In a closed system with two compartments the change in temperature has to be of opposite sign in the two compartments. Based on that argument, the ocean should cool when the atmosphere warms, because the total energy is conserved. This argument is inappropriate, however, because the climate system is an open system. The total energy content of the Earth can change because the longwave radiation emitted to space can vary, and so does the incoming energy due to changes in the global albedo. Nevertheless, the question is interesting: can we learn something about the cause of warming from the ocean and atmosphere temperature covariance? Is the ocean with its large heat capacity driving the atmosphere in a climate without external forcing, or is the ocean simply integrating the atmospheric signal?

<sup>1</sup>Institute for Atmospheric and Climate Science, ETH Zurich, Zurich, Switzerland.

Corresponding author: J. Sedláček, Institute for Atmospheric and Climate Science, ETH Zurich, Universitätsstr. 16, CH-8092 Zürich, Switzerland. (jan.sedlacek@env.ethz.ch)

©2012. American Geophysical Union. All Rights Reserved.  
0094-8276/12/2012GL053262

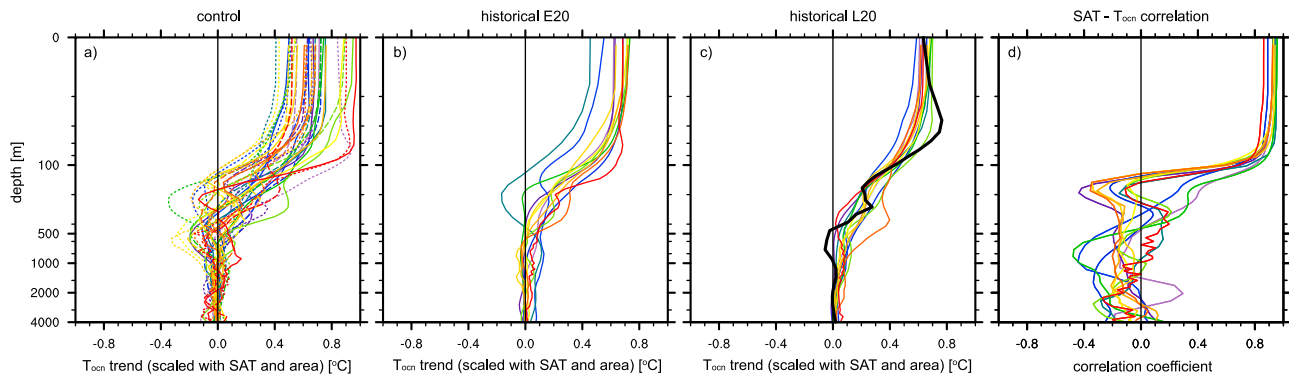


**Figure 1.** (a–c) The 50-yr ocean temperature trends for the control periods (Figure 1a), the early 20th-century periods (E20; Figure 1b), and the late 20th-century periods (L20; Figure 1c). (d) The correlation of SAT with the ocean temperature for the control simulations. Note that the temperature profiles are area weighted and in panels a–c scaled additionally with the global SAT trends. The colors denote the different models. Solid, dashed and dotted lines in panel a mark the periods with the largest, second largest, and third largest control SAT trend. The black line in panel c represents the temperature trend between 1955 and 2004 from SODA scaled with the NCEP/NCAR SAT trend.

[5] Observations of the last decades show a warming of the ocean [Domingues *et al.*, 2008; Levitus *et al.*, 2012] and the atmosphere [e.g., Morice *et al.*, 2012]. But can a forced warming be distinguished from changes due to natural unforced variability based only on patterns of warming in the ocean? While the large scale pattern of warming in the ocean is significant and well understood, only few studies have applied formal attribution techniques to the ocean warming [Barnett *et al.*, 2005; Palmer and Haines, 2009; Palmer *et al.*, 2007; Pierce *et al.*, 2006]. Until a few years ago, large uncertainties in ocean observations and discrepancies between the magnitude of internal variability in models and observations proved to be problematic [AchutaRao *et al.*, 2006; Gregory *et al.*, 2004]. Newer datasets agree much better with models incorporating all forcings [Domingues *et al.*, 2008], and suggest that the fingerprint attribution for the ocean is robust [Gleckler *et al.*, 2012].

[6] In this study we investigate whether there are signals or patterns of change which distinguish forced signals from natural variability and which can be understood physically, thereby complementing but not replacing the existing evidence and lines of arguments.

## 2. Method

[7] We use pre-industrial control simulations (no external forcing) and the 20th-century simulations (termed “historical”) of the World Climate Research Programme (WCRP) Climate Model Intercomparison Project Phase 5 (CMIP5) [Taylor *et al.*, 2012]. Twelve models provide the necessary data for the two simulation setups (bcc-csm1-1, CanESM2, CCSM4, CNRM-CM5, CSIRO-Mk3-6-0, GFDL-ESM2G, GFDL-ESM2M, IPSL-CM5A-LR, MPI-ESM-LR, MPI-ESM-MR, MPI-ESM-P, NorESM1-M). These models provide a total of 9353 yr of control simulations, and for each model the control simulation is at least 500 yr long. From these control simulations we select the three non-overlapping periods of 50 yr for every model with the largest surface air temperature (SAT) trends, resulting in a total of 36 periods with a substantial warming trend.

[8] Similar as for the control simulations we select the two non-overlapping periods of 50 yr each with the largest trends for each historical simulation. The period with the largest SAT slope is typically at the end of the 20th-century (L20), while the period with the second largest trend is during the early 20th-century (E20). So we have 36 periods of 50 yr with global surface warming caused by internal variability only (since the control simulations have no external forcing) and 24 periods where external forcing and internal variability contribute to the warming.

[9] All the results presented are scaled by the global SAT trend of the corresponding period in order to remove differences in magnitude, i.e. we focus on patterns of variability and change in this analysis. Some results based on unscaled data are discussed in the auxiliary material.<sup>1</sup> The vertical profiles are area weighted, i.e. the area-weighted temperature is proportional to the heat uptake in a unit layer and the integral over the whole depth is proportional to the total heat uptake.

## 3. Results

[10] Unlike in a closed system where one reservoir warms when the other is cooling, the global total ocean heat content and atmosphere temperatures in fact vary largely in phase. Indeed, the models used in this study show a positive correlation of 0.51 to 0.86 between the SAT and the ocean heat content integrated over the upper 300 m without external forcing. This indicates that the simultaneous warming of these two reservoirs tells us little about the cause of warming. On a multi-decadal time scale the changes in SAT and ocean heat content seem to be in phase down to 700 m depending on the model (see Figure S1 of the auxiliary material). In the historical, especially in the late 20th-century, the changes are in phase throughout the whole ocean.

[11] As shown in the normalized warming trends versus depth in Figure 1a, in all of the selected control segments with warming in the atmosphere, the ocean also warms in

<sup>1</sup>Auxiliary materials are available in the HTML. doi:10.1029/2012GL053262.

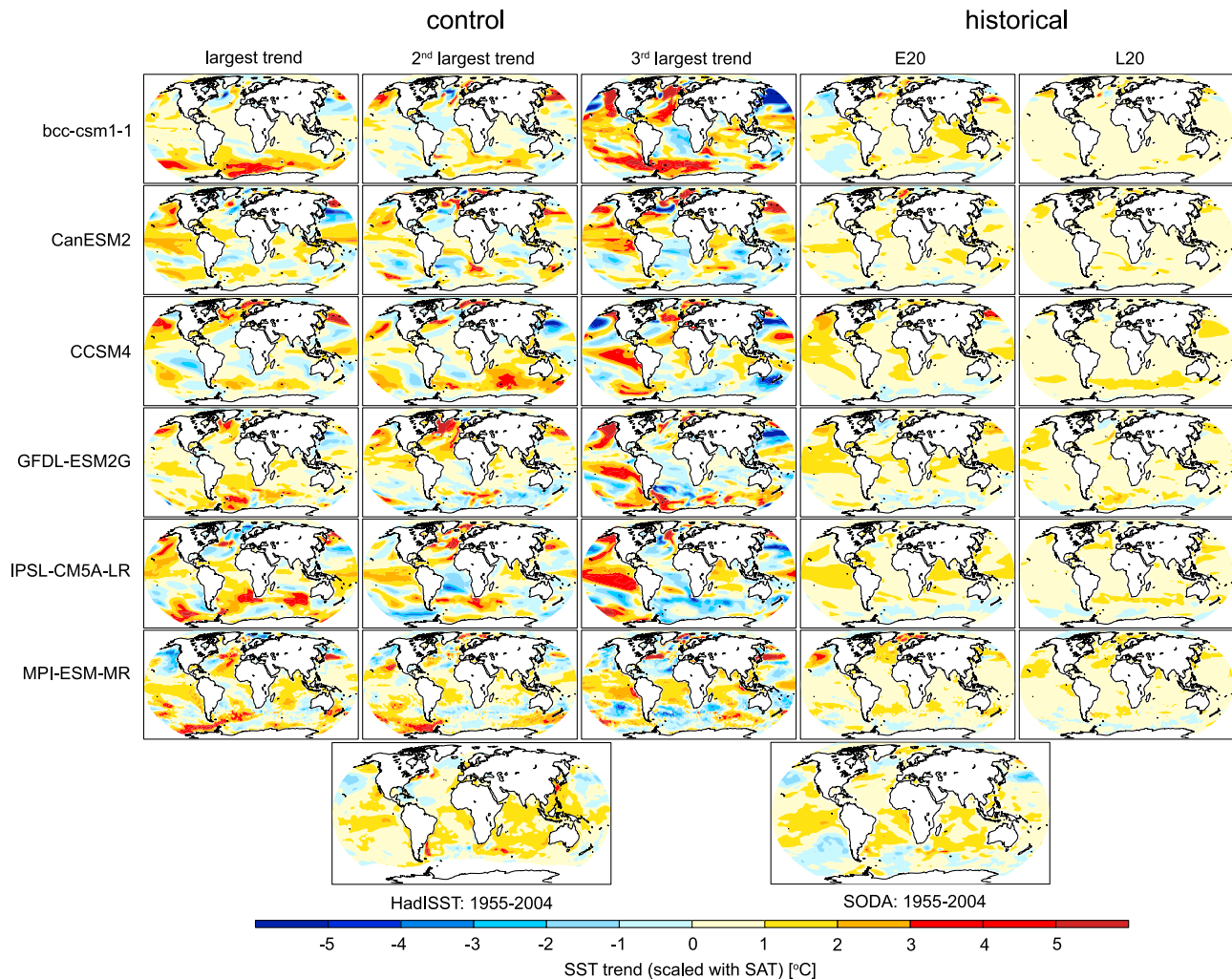


**Figure 2.** Sea surface temperature (SST) trends scaled with global surface air temperature (SAT) trends for a subset of the models used in this study. The first three columns show the control periods, column four the early 20th-century period (E20), and the fifth column the late 20th-century period (L20). The 1955 to 2004 HadISST and SODA SST trends scaled with global NCEP/NCAR SAT trends are shown at the bottom. Note that only half of the models used in this study are shown. The other half is shown in Figure S4 of the auxiliary material.

each individual layer in the top few hundred meters (i.e. not only in the 300 m average). In the 20th-century simulations (Figures 1b and 1c) the top 100 m behave similarly, but from about 100–500 m most forced simulations show positive trends, whereas the unforced simulation trends can be of either sign in the different control segments. While the 20th-century profiles fall within the envelope spanned by the control variability due to the normalization, they do not look like any individual realization of the control variability. The latter shows heterogeneous changes at different depth, while the L20 is smooth and almost monotonously decreasing with greater depth. As shown in Figure 1d the correlation between the SAT change and the ocean temperature is high and positive in the mixed layer down to about 100 to 200 m in the control runs. Below the mixed layer the ocean temperature and SAT trends are unrelated, consistent with Figure 1a.

[12] We analyzed lag correlation in the control simulations to understand whether the atmosphere is driving long-term changes in the ocean below the mixed layer or vice versa, and found that to be highly model dependent. In some models the ocean tends to lead the atmosphere, in others it lags (not

shown). The reasons for that are unclear, and the observational record is too short to evaluate the models. Also shown in panel 1c are the trends from 1955 to 2004 from SODA (Simple Ocean Data Assimilation) [Carton and Giese, 2008] scaled with the NCEP/NCAR SAT trend (National Centers for Environmental Prediction/National Center for Atmospheric Research) [Kalnay et al., 1996].

[13] The distribution of the warming with depth (without arguing about the overall magnitude) is consistent with a strong surface signal that is propagating slowly towards deeper layers by advection and diffusion, and is very similar in the 20th-century simulations and the observations. We argue that the change from a heterogeneous temperature trend profile (Figure 1a) to a more homogeneous one (Figures 1b and 1c) reflects the difference between natural variability and the forced signal. While the warming of the mixed layer is a simple consequence of the tight coupling between the atmosphere and surface ocean, the clear observed warming trends in intermediate depth layers (100–500 m) are a strong argument for an external forcing. Another interesting point is that the normalized warming in the topmost tens of meters

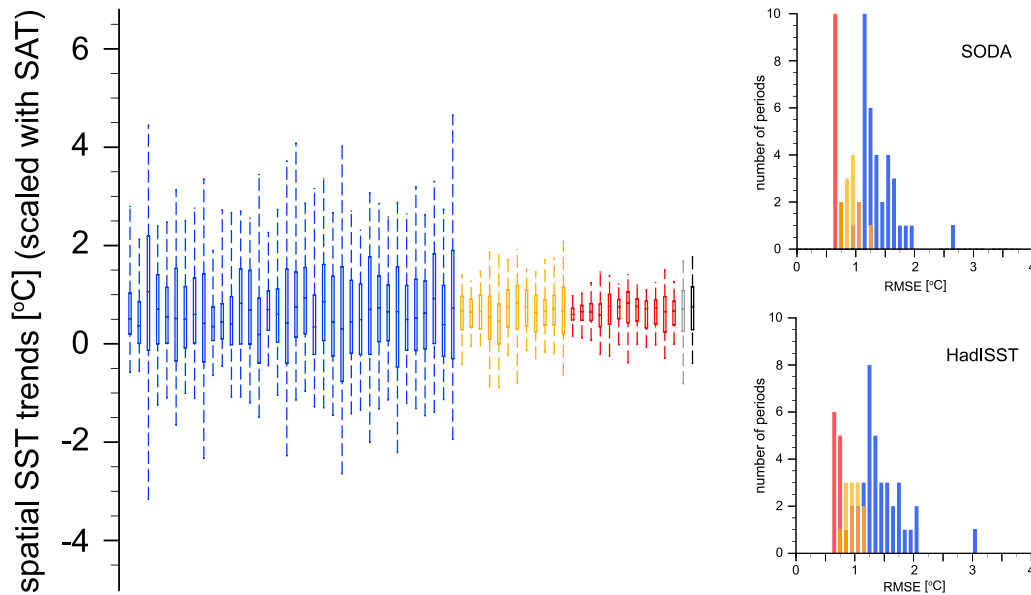


**Figure 3.** Spatial variability of the SST trends (area weighted) scaled with the global SAT trends. The boxplots denote the 5%, 25%, 50%, 75%, and 95% values of the distribution. The two insets show the root mean square error (RMSE) between the normalized patterns of the models and HadISST and SODA, respectively. The blue color denotes the 36 control periods, yellow the early 20th-century periods (E20), and red the late 20th-century periods (L20). Grey and black denote the data from SODA and HadISST (scaled with the global NCEP/NCAR SAT trends), respectively.

(relative to the global SAT trend) is very similar in all L20 simulations (about  $0.75^{\circ}\text{C}$ ) and within a few percent of the observations. This reflects the land-ocean contrast of the observed warming which is very robustly simulated in all models [Drost *et al.*, 2011]. For the control segments, however, the warming in that layer varies in a wide range ( $0.4$ – $0.9^{\circ}\text{C}$ ).

[14] Forest *et al.* [2008] found that the models participating in CMIP3 overestimated the deep-ocean heat uptake. This might also be the case in the CMIP5 model suite and this could explain part of the smooth changes with depth. However in our analysis the models used in the control and historical periods are the same. Thus even if the CMIP5 models were too diffuse our conclusions would remain similar. In addition, uncertainties in ocean observations are still substantial, in particular in deeper layers, and interpolation from sparse data could affect the estimated variability. Judging which models are more realistic is therefore difficult.

[15] The above conclusion is based only on patterns, since each 50-yr phase is normalized by the global SAT trend. A simple way to differentiate between a forced and an unforced signal is of course to argue based on the magnitude of the trend of the SAT and ocean temperature. Indeed the mean SAT trend of the late 20th-century trends (L20) is about 4 times larger than the mean of the largest trend of the control period and the smallest SAT trend from L20 is still about 1.6 times larger than the largest slope of the control period. The absolute trends of ocean heat content for the control simulations are shown in Figure S3 of the auxiliary material and are much smaller than those of the 20th-century simulations. These conclusions are similar to those by Huber and Knutti [2011] based on CMIP3. Our main point here, however, is that arguing about magnitudes relies on the assumption that climate models do not underestimate decadal variability, whereas the normalized warming profiles in Figure 1 provide support for an external

forcing based only on the depth profile, without knowing the magnitude of change. Note that the models used are the same for the control and historical periods and thus have the same unforced variability.

[16] We investigated if changes of the meridional overturning circulation (MOC) could have brought the heat from the surface to the deeper layers and smoothed the vertical temperature profile. However, the MOC was rather constant over the investigated periods and was not causing an additional warming of the deep layers.

[17] Is a homogeneous warming trend also visible in the surface fields? Indeed, Figure 2 (and Figure S4 of the auxiliary material) shows the normalized sea-surface temperature (SST) trend patterns to be much more ‘patchy’ in the control periods as compared to the historical periods. A few very warm regions mainly cause the warming in the control periods while in the historical simulations the changes in SST are much smoother. While the (largely forced) late 20th-century trend patterns in the models look similar to the observed pattern, none of the control segments exhibits such a homogeneous warming. This difference in spatial variability is summarized in Figure 3, showing box plots of local surface trends in each of the 50-yr periods. While in the control periods the range of spatial variability is about  $3$ – $6^{\circ}\text{C}$ , in E20 it is reduced to about  $2$ – $3^{\circ}\text{C}$ . The variability of the L20 periods, finally, is reduced to about  $1$ – $2^{\circ}\text{C}$ . On a closer look one might argue that the L20 periods are smoother than observed, as is the case in the vertical profiles. However, a root mean square error (RMSE) analysis between the model simulations and the observed fields shows that the L20 periods still agree better with observations than the E20 periods (see Figure 3 insets). The periods of the control simulations show the largest RMSE compared to observations. These conclusions are valid for HadISST and SODA.



[18] We also investigated if changes of the Atlantic Meridional Oscillation (AMO) or Pacific Decadal Oscillation (PDO) could explain the SST warming of the historical periods but found no evidence in the models. Indeed an EOF (Empirical Orthogonal Function) analysis of the control and E20 periods shows that the PDO and ENSO (El-Niño-Southern Oscillation) are the dominant modes of variability (not shown). While these two modes are still present in the L20 periods a new mode emerges as the main pattern. This pattern is very smooth and looks very similar to the HadISST and SODA SST trends shown in Figure 2. It reflects the fact that the change due to the forced signal has a different magnitude in the different models.

#### 4. Discussion and Conclusion

[19] In this study we have used CMIP5 model results to investigate forced vs. unforced coupled atmosphere-ocean changes. The SAT trends and ocean temperature trends in the historical simulations with anthropogenic forcing are much larger than trends due to internal variability found in 50-yr segments of unforced control simulations. But even if the patterns are normalized by the global SAT trends to account for the fact that models might underestimate internal variability, important distinctions remain. The forced simulations show a much more homogeneous warming spatially, and a smooth downward propagation of the warming signal to intermediate depth that is very similar to the observed ocean warming, but unlikely to be consistent with patterns found in the control periods. The method and results presented here do not directly provide a fraction of warming attributable to human influence like the optimal fingerprint methods, and can only separate internal variability from external drivers. But the idea is simple and transparent, based on physical understanding, and the combined evidence of atmosphere and ocean is taken into account. The patterns of warming from the forced simulations agree well with observations, and can easily be explained by known processes of advection and diffusion which propagate the surface warming to deeper layers in the ocean. Overall, they strongly support the conclusion from optimal fingerprint studies that the late 20th-century warming trend is to a large extent externally forced and not the result of internal ocean-atmosphere interactions.

[20] **Acknowledgments.** We acknowledge the World Climate Research Programme's Working Group on Coupled Modelling, which is responsible for CMIP, and we thank the climate modeling groups for producing and making available their model output. For CMIP the U.S. Department of Energy's Program for Climate Model Diagnosis and Intercomparison provides coordinating support and lead development of software infrastructure in partnership with the Global Organization for Earth System Science Portals.

[21] The Editor thanks the two anonymous reviewers.

#### References

- AchutaRao, K. M., B. D. Santer, P. J. Gleckler, K. E. Taylor, D. W. Pierce, T. P. Barnett, and T. M. L. Wigley (2006), Variability of ocean heat uptake: Reconciling observations and models, *J. Geophys. Res.*, **111**, C05019, doi:10.1029/2005JC003136.
- Barnett, T. P., D. W. Pierce, K. M. AchutaRao, P. J. Gleckler, B. D. Santer, J. M. Gregory, and W. M. Washington (2005), Penetration of human-induced warming into the world's oceans, *Science*, **309**(5732), 284–287, doi:10.1126/science.1112418.
- Booth, B. B. B., N. J. Dunstone, P. R. Halloran, T. Andrews, and N. Bellouin (2012), Aerosols implicated as a prime driver of twentieth-century North Atlantic climate variability, *Nature*, **484**(7393), 228–232, doi:10.1038/nature10946.
- Carton, J. A., and B. S. Giese (2008), A reanalysis of ocean climate using Simple Ocean Data Assimilation (SODA), *Mon. Weather Rev.*, **136**(8), 2999–3017, doi:10.1175/2007MWR1978.1.
- DeSole, T., M. K. Tippett, and J. Shukla (2011), A significant component of unforced multidecadal variability in the recent acceleration of global warming, *J. Clim.*, **24**(3), 909–926, doi:10.1175/2010JCLI3659.1.
- Domingues, C. M., J. A. Church, N. J. White, P. J. Gleckler, S. E. Wijffels, P. M. Barker, and J. R. Dunn (2008), Improved estimates of upper-ocean warming and multi-decadal sea-level rise, *Nature*, **453**(7198), 1090–1093, doi:10.1038/nature07080.
- Drost, F., D. Karoly, and K. Braganza (2011), Communicating global climate change using simple indices: An update, *Clim. Dyn.*, **39**, 989–999.
- Forest, C. E., P. H. Stone, and A. P. Sokolov (2008), Constraining climate model parameters from observed 20th century changes, *Tellus, Ser. A*, **60**(5), 911–920, doi:10.1111/j.1600-0870.2008.00346.x.
- Gleckler, P. J., et al. (2012), Human-induced global ocean warming on multidecadal timescales, *Nat. Clim. Change*, **2**(7), 524–529.
- Gregory, J. M., H. T. Banks, P. A. Stott, J. A. Lowe, and M. D. Palmer (2004), Simulated and observed decadal variability in ocean heat content, *Geophys. Res. Lett.*, **31**, L15312, doi:10.1029/2004GL020258.
- Hasselmann, K. (1979), On the signal-to-noise problem in atmospheric response studies, in *Meteorology Over the Tropical Oceans*, edited by B. B. Shaw, pp. 251–259, R. Meteorol. Soc., London.
- Hegerl, G. C., F. W. Zwiers, N. P. Braconnot, N. P. Gillett, Y. Luo, J. A. M. Orsini, N. Nicholls, J. E. Penner, and P. A. Stott (2007), Understanding and Attributing Climate Change, in *Climate Change 2007: The Physical Science Basis: Contribution of Working Group I to the Fourth Assessment Report of the Intergovernmental Panel on Climate Change*, edited by S. Solomon et al., pp. 663–745, Cambridge Univ. Press, New York.
- Huber, M., and R. Knutti (2011), Anthropogenic and natural warming inferred from changes in Earth's energy balance, *Nat. Geosci.*, **5**(1), 31–36, doi:10.1038/ngeo1327.
- Huss, M., M. Funk, and A. Ohmura (2009), Strong Alpine glacier melt in the 1940s due to enhanced solar radiation, *Geophys. Res. Lett.*, **36**, L23501, doi:10.1029/2009GL040789.
- Kalnay, E., et al. (1996), The NCEP/NCAR 40-year Reanalysis Project, *Bull. Am. Meteorol. Soc.*, **77**(3), 437–471, doi:10.1175/1520-0477(1996)077<0437:TNYRP>2.0.CO;2.
- Knutti, R., and G. C. Hegerl (2008), The equilibrium sensitivity of the Earth's temperature to radiation changes, *Nat. Geosci.*, **1**(11), 735–743, doi:10.1038/ngeo337.
- Levitus, S., et al. (2012), World ocean heat content and thermocline sea level change (0–2000 m), 1955–2010, *Geophys. Res. Lett.*, **39**, L10603, doi:10.1029/2012GL051106.
- Morice, C. P., J. J. Kennedy, N. A. Rayner, and P. D. Jones (2012), Quantifying uncertainties in global and regional temperature change using an ensemble of observational estimates: The HadCRUT4 data set, *J. Geophys. Res.*, **117**, D08101, doi:10.1029/2011JD017187.
- Palmer, M. D., and K. Haines (2009), Estimating oceanic heat content change using isotherms, *J. Clim.*, **22**(19), 4953–4969, doi:10.1175/2009JCLI2823.1.
- Palmer, M. D., K. Haines, S. F. B. Tett, and T. J. Ansell (2007), Isolating the signal of ocean global warming, *Geophys. Res. Lett.*, **34**, L23610, doi:10.1029/2007GL031712.
- Pierce, D., T. Barnett, K. M. AchutaRao, P. J. Gleckler, J. M. Gregory, and W. M. Washington (2006), Anthropogenic warming of the oceans: Observations and model results, *J. Clim.*, **19**(10), 1873–1900, doi:10.1175/JCLI3723.1.
- Swanson, K. L., G. Sugihara, and A. A. Tsonis (2009), Long-term natural variability and 20th century climate change, *Proc. Natl. Acad. Sci. U. S. A.*, **106**(38), 16,120–16,123, doi:10.1073/pnas.0908699106.
- Taylor, K. E., R. J. Stouffer, and G. A. Meehl (2012), An overview of CMIP5 and the experiment design, *Bull. Am. Meteorol. Soc.*, **93**(4), 485–498, doi:10.1175/BAMS-D-11-00094.1.